Insights into the Mechanism of the Benzoannelated Thieno[3,2-b]furan Halogenation. The Importance of HOMO-HOMO Interaction.

ARTICLE *in* THE JOURNAL OF PHYSICAL CHEMISTRY A · AUGUST 2013

Impact Factor: 2.69 · DOI: 10.1021/jp402257u · Source: PubMed

1 AUTHOR:

Ausra Vektariene
Vilnius University
30 PUBLICATIONS **170** CITATIONS

SEE PROFILE

THE JOURNAL OF PHYSICAL CHEMISTRY A

Article

pubs.acs.org/JPCA

Insights into the Mechanism of the Benzoannelated Thieno[3,2-*b*]furan Halogenation. Importance of HOMO−HOMO Interaction

Ausra Vektariene*

Institute of Theoretical Physics and Astronomy, Vilnius University, A. Gostauto 12, LT-01108 Vilnius, Lithuania

ABSTRACT: In this paper the mechanism of the benzoannelated thieno[3,2-*b*]furan halogenation reaction has been characterized using density functional theory calculations. The solvent effect on the studied reaction is taken into account. A variation in charge, bond length, and bond order in the transformation of the π-complex to the σ-complex and final products along the reaction minimal energy path given as the intrinsic reaction coordinate has been investigated. Particular attention was focused on the evolution of π MOs along the reaction coordinate. The importance of HOMO−HOMO interaction between the lone pair electrons of the bromine molecule and π MOs of thieno[3,2-*b*]benzofuran has been emphasized.

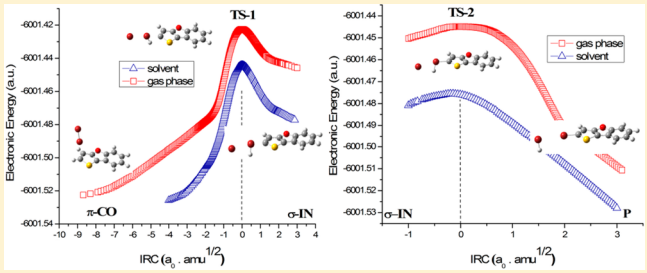

1. INTRODUCTION

Aromatic electrophilic substitution (Ar-ES) reactions of benzofused electron-rich five-membered heterocycles are among the most thoroughly studied reactions in organic chemistry owing to their wide range of applications in material sciences and medicine.[1−11] Materials containing substituted electron-rich five-membered heterocycles are successfully applied to the design of novel liquid crystals.[12,13] Many experimental works dealing with an attempt to obtain halogenated electron-rich five-membered heterocycles have been extensively developed in this field.[14,15] Moreover, the experimental studies have been carried out to clarify the nature of the electrophilic substitution reaction in these heterocycles.[14−16] It was suggested that electrophilic substitution in the simple five-membered heterocycles furan and thiophene occurs with positional selectivity and via the aromatic σ-complex.[14−18] More recently Domingo et al. rationalized the relative reactivities of five-membered heterocycles in electrophilic aromatic substitution reaction by means of the global nucleophilicity index.[19−22] Later Gromri et al. extended this investigation and has shown that the experimental trends of the relative reactivities and regioselectivities of these reactions can be correctly predicted using calculated global nucleophilicity reactivity indices.[23] Mineva reported and discussed the reactivity descriptors of thiophene, furan, and pyrrole using Fukui indices.[24] Svoboda et al. investigated electrophilic substitution reactions of more complicated benzofused five-membered heterocycles.[12,25,26] By applying NMR spectroscopy, it was assumed that the bromination reaction of thieno[3,2-*b*]benzofuran proceeds via the aromatic electrophilic substitution scenario. Recently we extended this experimental study by means of theoretical investigation.[27] Using the density functional theory (DFT) based on the global and local quantum chemistry reactivity descriptors approach, we suggested that the delocalized π-electron surface of thieno[3,2-*b*]benzofuran consists of a stable aromatic system between the benzene ring and the electron-rich thiophene heterocycle. Consequently, an aromatic electrophilic substitution mechanism scenario for thieno[3,2-*b*]benzofuran has been assumed. However, the whole course of electrophilic aromatic substitution between the bromine molecule and thieno[3,2-*b*]benzofuran is still unclear. Moreover, at first sight the Ar-ES of bromine molecule with electron-rich five-membered heterocycles is an exciting process because it allegedly involves the interaction of two nucleophilic species. The reaction typically occurs with the bromide molecule bearing six lone pairs of electrons that tend to increase apparent nucleophilicity and the heterocycle bearing a heteroatom with an electron pair conjugated to the aromatic π-electron system that is delocalized over the ring.

In this paper, we further explore the bromination reaction mechanism of thieno[3,2-*b*]benzofuran by means of reaction potential energy profile estimation.[25−27] Based on the selected model, an attempt was made to illuminate the charge and bond character changes in the transformation from π-complex to σ-complex. The frontier π molecular orbital (MO) energy level splittings and shape mixing during the π-complex formation and transformation into the π-complex along the reaction minimal energy path given as the intrinsic reaction coordinate has been described. The significance of the highest occupied molecular orbital (HOMO)−HOMO interaction between the

Received: March 5, 2013
Revised: July 30, 2013
Published: August 1, 2013

dx.doi.org/10.1021/jp402257u | *J. Phys. Chem. A* 2013, 117, 8449−8458

lone pair electrons on the bromine atom and π MOs of thieno[3,2-*b*]benzofuran has been discussed.

2. THEORETICAL BACKGROUND AND COMPUTATIONAL DETAILS

The classical approach widely used to explain reaction mechanisms is calculations of the reaction potential energy (or free energy) surface based on the transition state theory (TST).[28] According to the fundamental assumption of TST, the evolution of the potential energy is associated with the minimal energy reaction path, connecting the stationary points (reactants, products, intermediates, and transition states). The characterization of stationary points on the reaction minimal energy path (MEP) offers a clearer view of chemical trends of the pending reactions. In this article, the reaction mechanism has been described as a structural evolution defined by the changes in the electron population on the π molecular orbitals during the reaction progress given as the intrinsic reaction coordinate (IRC).[29,30] For this purpose the frontier molecular orbital theory (FMO) and perturbation molecular orbital theory (PMO) approaches were used to estimate the π molecular orbital transformations on the reaction MEP.[31−33]

The most commonly used two electron FMO theory applications[31−33] rely on the fact that the extent of initial HOMO−lowest unoccupied molecular orbital (LUMO) interactions is inversely proportional to the separation of HOMO and LUMO energies of reacting species. The large energy gap between frontier orbitals of reactants is associated with a high reaction activation energy barrier and either a low reaction rate or reaction cessation.

However, Bach and Wolber et al. described[34] conditions under which certain reactions where reactants have a large initial HOMO−LUMO energy gap (>100 kcal/mol) can proceed with comparatively low activation energies. Analyzing this phenomenon, they emphasized the importance of a four electron HOMO−HOMO interaction in lowering of the reaction activation barrier[35−38] and considered how the transition state can be determined by the interplay of two electron HOMO−LUMO and four electron HOMO−HOMO interactions. The possibilities of four electron HOMO−HOMO interaction were discussed in terms of PMO.[31,34−40] The basic two and four electron molecular orbital interactions that will affect the energetics of reacting system are illustrated in Figure 1 by the simplified molecular hydrogen and ethene interaction model. In two electron HOMO−LUMO interaction the HOMO π orbital of the nucleophile (ethene) mixes with the LUMO orbital of the electrophile (hydrogen molecule) in a bonding way affording the highest filled orbital of the transition state or metastable reaction complex π+electrophile* (elect*) combination that is reduced in energy with the stabilizing effect on the system. The mixing of the LUMO orbital of the electrophile and the π orbital of the nucleophile in an antibonding way affords the π−elect* vacant orbital combination, which is elevated in energy.

By the four electron interaction model the π HOMO of the nucleophile mixes with the HOMO orbital of the electrophile in an antibonding way affording the π−elect filled combination elevated in energy. The mixing of the nucleophile π and electrophile HOMOs in a bonding way provides the π+elect filled orbital combination, which is reduced in energy, stabilizing the highest antibonding π−elect combination effect. Thus, the four electron interaction is responsible for elevation of the HOMO closer to the LUMO level and may also be

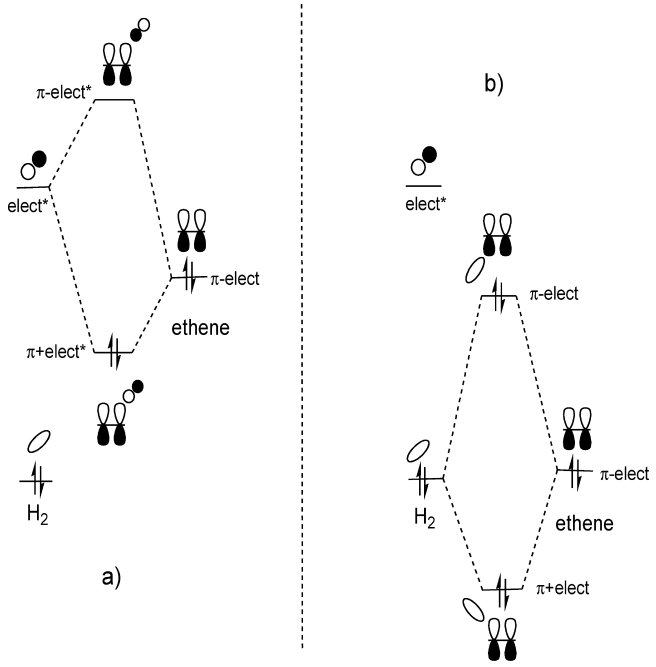

Figure 1. (a) Two electron and (b) four electron orbital interactions involved in the molecular hydrogen electrophilic addition to ethene.

accompanied by a lowering of the LUMO along the reaction coordinate. This interaction is responsible for the magnitude of the activation energy and is fundamental for the understanding of the derivation of resultant MOs in the reaction transition states.[31,34−40] In this manner one can understand how reactions with a large initial HOMO−LUMO gap can proceed at comparatively low activation energies. Therefore, if the four electron orbital interaction can progress, the magnitudes of atomic orbital coefficients of HOMOs should be reflected in orbital mixing.

All the calculations were performed with the Gaussian 03 suite of programs.[41] The DFT methods, particularly the Becke, three-parameter, Lee−Yang−Parr functional (B3LYP),[42−48] have been successfully used in the theoretical understanding of heterocyclic molecules. This B3LYP method has recently been reported to yield excellent results for the prediction of reactivity and electronic structure of complicated partially bonded ionic heterocyclic species.[43,46−49] Therefore, in this study we chose the B3LYP method for geometry optimizations and frequency calculations. Also, a certain consideration was taken into account choosing an appropriate basis set for the current study. An attempt to choose basis sets 6-311++G(d, p), 6-31+G(d), 6-31G(d, p), and 6-31G(d) for evaluation of reactions of heterocyclic systems with heavy atoms revealed that all basis sets provided almost identical results.[49−51] Thus, the 6-31G(d) basis set should be the best compromise between speed and accuracy for reactions involving the interactions with bromine atom. It is worth mentioning that Pople et al. have extended the medium basis sets 6-31G and 6-31G(d) for the third-row elements including bromine.[41,52] The extended 6-31G basis set has six primitive Gaussians for 1s, 2s, 2p, 3s, and 3p orbitals, and a split-valence pair of three and one primitives for valence orbitals, which are 4s, 4p, and 3d. Also, the polarization functions for the third-row atoms including bromine were renewed. The extended 6-31G and 6-31G(d) basis sets were implemented to Gaussian 03.[41,52] Furthermore, Pople et al. performed a number of geometry optimization

dx.doi.org/10.1021/jp402257u | J. Phys. Chem. A 2013, 117, 8449−8458

calculations with the renewed 6-31G and 6-31G(d) basis sets for a number of compounds, among which were compounds bearing bromine atoms, and concluded that computational results were in close agreement with the experimental data.[52] Hereafter, Poirier et al. found that calculation of reaction energetics obtained using the standard 6-31G and 6-31G(d) basis sets for the reactions of bromine with alkenes and isogyric reactions involving bromine showed close agreement with experimental data as compared to the calculations with Binning−Curtiss (BC6-31G) basis sets.[53]

Because the reaction of bromine with certain heterocycles is known to proceed through the formation of charged or ionic species,[14] the diffuse functions were added to the standard 6-31G(d) basis set and the B3LYP/6-31+G(d) level of theory was considered for the outlined calculations. The Gibbs free energies at 298 K and 1 atm and electronic energies with the zero-point-energy correction for the reaction stationary points have been calculated. Each determined energy minimum and the saddle point were confirmed by the frequency calculations. Transition states were located using the linear synchronous transit method.[54] Frequency calculations were performed following each optimization to characterize all stationary points located on the potential energy profile. Moreover, single-point energies were calculated at the B3LYP/6-31++G(d,p) level using the B3LYP/6-31+G(d) optimized geometries. Solvent effects were modeled using the integral equation formalism polarized continuum model (IEFPCM),[55−57] by means of geometry optimization and frequency calculation at the B3LYP/6-31+G(d) level.

IRC calculations were used to verify the connectivity of the transition states to intermediates or product via the reaction minimum energy paths.[58,59] Chemical bond disruption and formation were quantified by the Wiberg bond index, which reflects the superposition of electron density between two interacting atoms. A high Wiberg bond index indicates a strong covalent bonding interaction between the two relevant atoms. Charge distributions and the Wiberg bond indices were determined via natural bond orbital (NBO)[60] analysis at the B3LYP/6-31++G(d,p) level.

The electronic structure changes during the reaction progress have been investigated on the basis of Kohn−Sham (KS) molecular orbital theory. Recently Kohn−Sham density functional theory methods made their appearance as an alternative to the theoretical methods based on Hartree−Fock (HF) theory.[61−64] The KS DFT method combines a relatively high efficiency and accuracy and constitutes a plausible molecular orbital model.[65] This allows predicting the behavior of chemical reactivity, understanding of the electron-donating or electron-accepting interaction properties, and the chemical bond nature in terms of MO theory treatment.[31,65−67] Therefore, the molecular orbital concept at the DFT level and the behavior of HF and KS orbitals have been extensively analyzed and discussed for many molecules.[68−71] However, sometimes such discussions are objects of some controversy. Rodrigo et al. analyzed the acid−base behavior for a large number of compounds using HF and KS molecular orbitals.[72] They noted that HF and KS HOMO energies usable as descriptors for the pK_a values are inadequate in describing the acidities of these compounds. Therefore, they proposed the so-called frontier effective-for-reaction MO criterion to obtain a good correlation between the acidity and molecular orbital energies to drive the acid−base reactions.[72] Differently from observations in ref 72, Zevallos[73] evaluated the performance of the HF and KS orbital energies to produce electronic properties depending on the HOMO energy such as the ionization potential. The results obtained indicated that calculated electronic properties by means of DFT hybrid functionals lead to a good approximation to the experimental values of the ionization potential as compared to HF methods. Stowasser and Hoffmann[74] also made a comparison between HF and KS orbitals. They investigated which molecular orbital HF or KS is the best for describing the reactivity for a set of small molecules. Finally, they found that KS orbitals are suitable for qualitative MO analysis. The shape and symmetry properties of the KS orbitals have been found to be very similar to those calculated by HF.

3. RESULTS AND DISCUSSION

3.1. Reaction Energy and Structural Changes. The electrophilic bromination of thieno[3,2-*b*]benzofuran undergoes exclusive bromination with high regioselectivity of the C(2) atom on the thiophene ring.[25−27] The reaction was executed under mild reaction conditions using the aprotic poor polar solvent dichloromethane in the absence of catalyst. The reaction conditions should play a very important role in the stabilization of different intermediates and transition states. In the absence of catalyst the attacking bromine molecule can be polarized by the π-electron-rich aromatic ring system, using aprotic nonpolar solvents.[75−77] Thus, in this study, to simulate experimental conditions, we have modeled the reaction considering the dichloromethane solvent.

The schematic free energy profile and the optimized geometries of all stationary points along the reaction coordinate are shown in Figures 2 and 3. Electronic energy changes along

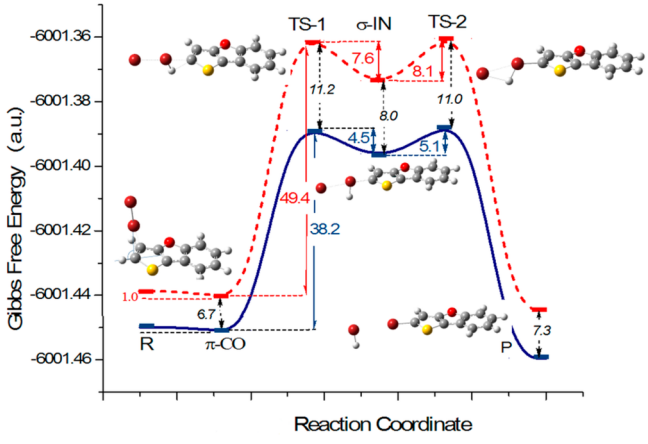

Figure 2. Schematic Gibbs free energy profile (au), in the gas phase (red dashed line) and solvent phase (blue solid line), for the thieno[3,2-*b*]benzofuran bromination reaction. The differences of Gibbs energies are presented in kcal/mol. Calculations were done at the B3LYP/6-31+G(d) level.

the IRC for the transition states TS-1 and TS-2 are presented in Figures 4 and 5. The important for study structural parameters are represented in Tables 1 and 2. The values of relative Gibbs free energies (ΔG) at 298 K and 1 atm, the relative electronic energies with zero-point-energy corrections for the reaction paths, and the imaginary frequency modes of TSs are collected in Table 3. The charge transfer of the reacting system is presented in Table 4.

dx.doi.org/10.1021/jp402257u | J. Phys. Chem. A 2013, 117, 8449−8458

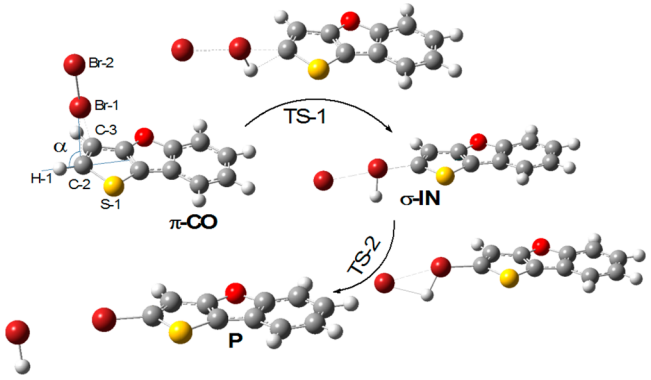

Figure 3. Structures of thieno[3,2-*b*]benzofuran bromination reaction stationary points: π-complex (π-CO), transition state (TS-1), σ-complex intermediate (σ-IN), transition state (TS-2), and reaction products (P). Calculations were done at the B3LYP/6-31+G(d) level.

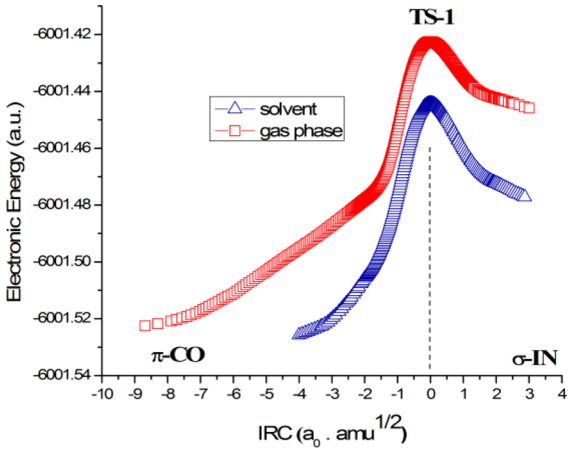

Figure 4. Electronic energy profile along the intrinsic reaction coordinate (IRC) for transition state TS-1. Calculated by IRC following the method at the B3LYP/6-31+G(d) level for the gas phase and solvent.

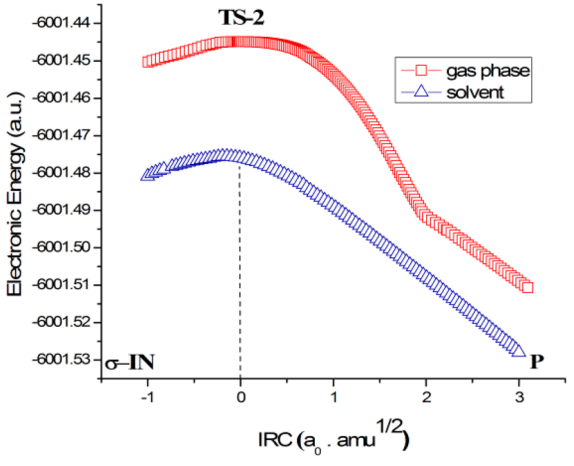

Figure 5. Electronic energy profile along the intrinsic reaction coordinate (IRC) for transition state TS-2. Calculated by IRC following the method at the B3LYP/6-31+G(d) level for the gas phase and solvent.

The reaction starts with the interaction of Br(1)−Br(2) and thieno[3,2-*b*]benzofuran under formation of a π complex (π-CO). This process leads to a slight decrease in energy. The thieno[3,2-*b*]benzofuran establishes a unique localized metastable π complex π-CO with the bromine molecule positioned over the rim of the thiophene ring. The π-CO complex adopts an oblique structure with Br(1)−Br(2) directed almost perpendicularly to the thieno[3,2-*b*]benzofuran plane. The Br(1) atom is facing the C(2) atom of the thiophene ring plane. The reacting C(2) atom is coplanar with the ring plane of thiophene and benzofuran rings. This indicates that the C(2) atom in the thiophene ring adopts hybridization sp^2, leaving a p orbital to conjugate with the π-electron system of the heterocycle. It acquires the most negative charge on the C(2) carbon atom as shown in Table 4. Moreover, the angle α in π-CO is close to 90° (94.3°) and the bond length $BL_{Br(1)-Br(2)}$ (2.38 Å) is longer than that of the bromine molecule, $BL_{Br(1)-Br(2)}$ (2.33 Å); the bond orders $BI_{C(2)-Br(1)}$ and $BI_{C(3)-Br(1)}$ are 0.09 and 0.03, respectively. These facts indicate a weak interaction between the Br(1) atom and the C(2) and C(3) atoms of the thiophene ring and suggest the existence of a weak nonsymmetric three-membered π complex in π-CO between the bromine and the C(2) and C(3) atoms with the bromine positioned over the rim of thiophene ring, and oriented perpendicular to the heterocycle plane.

As the system moves along the reaction coordinate to the transition state TS-1, essential structural changes occur. First, the Br(1)−Br(2) moiety migrates toward the thiophene ring with the bromine Br(1) atom directing toward C(2), and the angle α changes from 94.31 to 7.39°, which indicates that the interaction changes from π-bonding to a σ-bonding character. Second, $BL_{C(2)-Br(1)}$ shortens from 2.85 to 2.20 Å and the $BI_{C(2)-Br(1)}$ increases from 0.09 to 0.55 with the C(3)−Br(1) distance lengthening up to 3.2 Å. $BL_{Br(1)-Br(2)}$ is lengthened from 2.38 to 2.62 Å with the $BI_{Br(1)-Br(2)}$ weakening from 0.89 to 0.44, indicating the C(2)−Br(1) bond formation and the Br(1)−Br(2) bond breakup. Third, $BL_{H(1)-C(2)}$ is lengthened from 1.08 to 1.77 Å with the $BI_{H(1)-C(2)}$ weakening from 0.90 to 0.14, whereas $BL_{H(1)-Br(1)}$ is shortened strongly from 2.98 to 1.51 Å with the $BI_{H(1)-Br(1)}$ growing to 0.73, indicating the formation of a polarized C(2)−H(1)−Br(1) moiety and noticeable proton migration.

The transition of the complex π-CO to TS-1 requires a free activation energy of 49.4 kcal/mol. The calculation result presented here supports the experimental observations and testifies that the bromination process of the pending system is irreversible and proceeds slowly.[25,26] Behind this barrier, the system moves to the σ-intermediate (σ-IN). The energy of σ-IN is 41.8 kcal/mol higher compared to that of π-CO. The structure of σ-IN is analogous to that of TS-1, with $BL_{C(2)-Br(1)}$ shortened and $BL_{Br(1)-Br(2)}$ lengthened slightly at the transition state TS-1. The complete migration of the proton H(1) to Br(1), with $BL_{H(1)-Br(1)}$ of 1.44 Å and $BI_{H(1)-Br(1)}$ of 0.89, is the most significant change from TS-1 to σ-IN.

Further, the system can easily overcome the free energy barrier starting from σ-IN to the second transition state (TS-2), which produces the final product. The free energy barrier of the second step is 8.1 kcal/mol.

The ascendant structural change in the second step starting from σ-IN to TS-2 is the migration of the proton H(1) from the bromine Br(1) to Br(2). Therewith the bond length $BL_{H(1)-Br(1)}$ lengthens slightly from 1.44 to 1.45 Å and weakens $BI_{H(1)-Br(1)}$ from 0.89 to 0.85, whereas $BL_{H(1)-Br(2)}$ shortens from 2.78 to 2.26 Å and strengthens $BI_{H(1)-Br(2)}$ from 0.01 to 0.3. The Br(1)−Br(2) bond (2.79 Å) is remarkably weakened in TS-2 to $BI_{Br(1)-Br(2)}$ 0.25 suggesting the Br(2) atom and the

dx.doi.org/10.1021/jp402257u | J. Phys. Chem. A 2013, 117, 8449−8458

Table 1. Particular Structural Parameters of the Thieno[3,2-*b*]benzofuran Bromination Reaction: Bond Lengths (in Å) and *α* Angles (in deg) of Reaction Stationary Points in Gas Phase and in Solvent Phase (Values in Parentheses)[a]

geometry	R	*π*-CO	TS-1	*σ*-IN	TS-2	P
H(1)−C(2)	1.08(1.09)	1.08(1.09)	1.77(1.67)	2.56(2.63)	2.66(1.46)	5.53(5.61)
iBr(1)−C(2)	–	2.85(2.61)	2.20(2.08)	2.02(1.93)	2.00(1.92)	1.89(1.89)
Br(1)−Br(2)	2.33(2.33)	2.38(2.46)	2.62(2.83)	2.70(3.01)	2.79(3.05)	3.52(3.51)
H(1)−Br(1)	–	2.98(2.81)	1.51(1.53)	1.44(1.51)	1.45(1.46)	3.75(4.05)
H(1)−Br(2)	–	5.23(5.14)	3.66(3.92)	2.78(3.15)	2.26(2.70)	1.44(1.47)
α	–	94.31(78.06)	7.39(2.03)	5.71(1.54)	2.04(1.15)	0.01(0.01)

[a]Single point energy calculations at B3LYP/6-31++G(d,p) level for the optimized geometries at the B3LYP/6-31+G(d) level.

Table 2. Particular Structural Parameters: Wiberg Bond Order Index of the Thieno[3,2-*b*]benzofuran Bromination Reaction Stationary Points[a]

geometry	R	*π*-CO	TS-1	*σ*-IN	TS-2	P
H(1)-C(2)	0.91	0.9	0.14	0.01	0.01	0.00
Br(1)−C(2)	–	0.09	0.55	0.73	0.77	1.06
Br(1)−Br(2)	1.03	0.89	0.44	0.35	0.25	0.02
H(1)−Br(1)	–	0.00	0.73	0.89	0.85	0.00
H(1)−Br(2)	–	0.00	0.03	0.05	0.34	0.96

[a]Single point energy calculations at the B3LYP/6-31++G(d,p) level for the optimized geometries at the B3LYP/6-31+G(d) level.

Table 4. Natural Population Analysis Charges on Selected Atoms and Dipole Moments (*μ*, D) of the Thieno[3,2-*b*]benzofuran Bromination Reaction Stationary Points[a]

atom	R	*π*-CO	TS-1	*σ*-IN	TS-2	P
Br(1)	0.00	−0.03	0.36	0.55	0.54	0.14
Br(2)	0.00	−0.07	−0.44	−0.61	−0.64	−0.2
C(2)	−0.36	−0.38	−0.43	−0.41	−0.42	−0.37
S(1)	0.44	0.46	0.48	0.48	0.48	0.48
C(3)	−0.28	−0.27	−0.31	−0.29	−0.28	−0.29
H(1)	0.22	0.24	0.28	0.23	0.25	0.18
μ	0.36	2.72	7.31	8.98	9.77	2.59

[a]Calculations at the B3LYP/6-31++G(d,p) level.

H(1) proton interaction. The bromination is completed as the H(1) atom further migrates to Br(2) up to $BL_{H(1)-Br(2)}$ of 1.44 Å and $BI_{H(1)-Br(2)}$ of 0.96 and the products 2-bromothieno[3,2-*b*]benzofuran and HBr are finally formed.

The calculated reaction free energy profile shows that during this process a significant structural change involves a transfer of the H(1) atom from C(2) to Br(1) and finally to the Br(2) atom, accompanying the formation of the C(2)−Br(1) bond and breakage of the Br(1)−Br(2) bond in the bromine molecule. From *π*-CO to *σ*-IN, two bonds (C(2)−Br(1) and Br(1)−H(1)) are formed and two bonds (Br(1)−Br(2) and C(2)−H(1)) are broken. From *σ*-IN to the product, a dramatic decrease in the bond index of Br(1)−H(1) and an increase in that of Br(2)−H(1) happen during the conversion from TS-2 to the product, indicating that H(1) migration from Br(1) to Br(2) is involved in this process. By this route thieno[3,2-*b*]benzofuran and bromine produce two products: 2-bromothieno[3,2-*b*]benzofuran and HBr. The free energy profile (Figure 2) is similar to the energy profile of aromatic electrophilic substitution with bromine. A high energy barrier of the rate limiting step indicates a lower reactivity of this heterocyclic system. However, solvent effects may play an important role in reducing the energy barrier of the bromination reaction.

3.2. Solvent Effects. Solvent effects on the reaction stationary points were estimated by the integral equation formalism polarized continuum model (IEFPCM) method with the dichloromethane as solvent.[55−57] The Gibbs free energies and certain bond length values for reaction stationary points in the gas phase and in solvent are compared graphically and are presented in Figure 2. The bond lengths in angstroms and *α* angles in degrees of reaction stationary points in solvent phase are presented in Table 1. The relative Gibbs free energies and electronic energies with zero-point-energy corrections in the gas phase and solvated media selected for the reaction stationary points are given in Table 3. The dipole moments *μ* in debyes and charges obtained by natural population analysis are presented in Table 4.

The stationary points TS-1, *σ*-IN, and TS-2 exhibit a strong charge separation between the bromine atoms of the Br(1)−Br(2) unit and large dipole moments of 7.31, 8.98, and 9.47 for TS-1, *σ*-IN, and TS-2, respectively. This suggests that the stabilization of these stationary points can be strongly

Table 3. Calculated Relative Electronic Energies with Zero-Point Energy Corrections (Δ*E*) and Relative Gibbs Free Energies (Δ*G*) in kcal/mol for the Thieno[3,2-*b*]benzofuran Bromination Reaction Stationary Points in the Gas Phase and in Solvent[a,b]

	B3LYP/6-31+G(d)				B3LYP/6-31++G(d,p)	
	Δ*E*		Δ*G*		Δ*E*	
species	gas phase	solvent	gas phase	solvent	gas phase	solvent
R	0	0	0	0	0	0
π-CO	−5.33	−7.58	−0.65	−0.91	−7.09	−7.69
TS-1	42.07 (1145.1i)	32.92 (1276.9i)	48.75	38.14	38.28	24.46
σ-IN	30.81	25.15	40.97	33.7	27.30	23.93
TS-2	43.02 (277i)	29.31 (27.5i)	49.10	38.74	39.29	27.65
P	−9.03	−14.20	−3.69	−6.04	−14.18	−16.02

[a]The imaginary frequencies (cm^{-1}) of the transition structures are in parentheses. [b]Calculations at the B3LYP/6-31+G(d) level and single point energy calculations at the B3LYP/6-31++G(d, p) level.

dx.doi.org/10.1021/jp402257u | J. Phys. Chem. A 2013, 117, 8449−8458

influenced by the solvent. Meanwhile, the complex π-CO and the reaction product P do not express a strong charge separation effect and have small dipole moments equal to 2.72 and 2.59, respectively. This suggests that the solvation might have only a slight influence on the stabilization energy of the complex π-CO and the reaction product P. The comparison of calculated Gibbs free activation and stabilization energies in the gas phase and in solvent confirms this assumption, indicating that the solvation influenced stabilization of the transition states TS-1 and TS-2 as well as the intermediate σ-IN to a greater extent than the solvation influenced stabilization of the complex π-CO and product P. The decreased free activation energies for the solvent reaction conditions compared to the gas phase of TS-1 and TS-2 and the stabilization energy for σ-IN are 11.2, 11.0, and 8.0 kcal/mol, respectively. The free stabilization energies for the solvent reaction conditions of π-CO and P decrease by 6.7 and 7.3 kcal/mol, respectively. This means that the solvation can have a significant effect on the reduction of activation energy barriers and can facilitate the thieno[3,2-*b*]benzofuran bromination reaction.

3.3. Charge Transfer. The charges obtained by natural population analysis on the most important atoms for reaction progress are noted in Table 4 for all stationary points. As a result of the first step, the neutral Br(1)−Br(2) unit in π-CO approaches the transition state TS-1 and becomes polarized in σ-IN. Simultaneously, the positive charge on the Br(1) atom in the bromine unit increases gradually from −0.03 in π-CO to +0.35 in TS-1 and to +0.53 in σ-IN, whereas Br(2) becomes more negative along the same path. The positive charge is mainly located on the bromine Br(1) atom. The charge separation effect of bromine Br(1)−Br(2) shows itself in the first reaction step. Both TS-1 and σ-IN are of the same character similar to the bromoarenium cation specific to Ar-ES reactions. This charge separation weakens the Br(1)−Br(2) bond and causes a positive charge transfer from Br(1) to H(1) as the system goes from σ-IN to TS-2.

The charge separation remains large +0.54 for Br(1) and −0.64 for Br(2) until the system reaches TS-2. From TS-2 the negative charge of the Br(2) atom reduces, resulting in the negative charge flow from Br(2) to Br(1)···H(1) and simultaneous migration of H(1) from Br(1) to Br(2) and decrease in the positive charge in the bromine Br(1). The charge separation effect of the Br(1)−Br(2) unit in TS-1, σ-IN, and TS-2 implies that bromination may proceed via an ion pair route.

3.4. Molecular Orbital Interactions. The charge transfer and electron density migration along the reaction coordinate can also be elucidated through the evaluation of molecular orbital transformations along the MEP. In this article the bromine (Br) and thieno[3,2-*b*]benzofuran (TF) displacement reaction was first examined on the basis of the approach of the FMO and PMO theories. The KS molecular orbital shapes and their energies for the reaction stationary points were evaluated at the B3LYP/6-31++G(d,p) level. We assumed that the displacement reaction between bromine and thieno[3,2-*b*]-benzofuran involves an electrophilic bromine and nucleophilic thieno[3,2-*b*]benzofuran interaction as generally accepted in the mechanistic studies of the Ar-ES reaction. The relevant frontier orbitals involved in the prereacting complex π-CO formation are shown in Figure 6; further changes in the MO shapes and energies along the IRC are denoted in Figure 7.

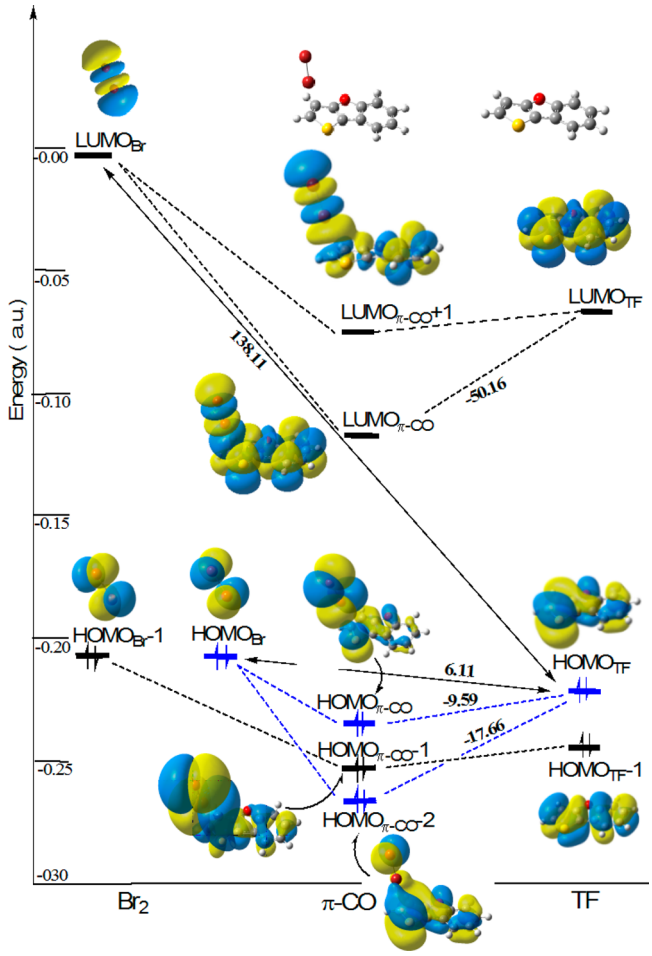

Figure 6. KS molecular orbital interaction diagram for π-complex (π-CO) formation stage of the thieno[3,2-*b*]benzofuran bromination reaction. KS orbital energy differences in kcal/mol. Single point energy calculations at the B3LYP/6-31++G(d,p) level for the optimized geometries at the B3LYP/6-31+G(d) level.

The bromine molecule has six lone pair electron (σ and π) molecular orbitals that differ in energy and shape. Figure 4 presents, for our study, the two most important highest occupied orbitals, HOMO$_{Br}$ and HOMO$_{Br}$ − 1, of bromine which correspond to antibonding degenerative π type (π_g) orbitals, and the LUMO$_{Br}$ orbital of bromine belongs to the lowest unoccupied antibonding σ type (σ_u) orbital. The relevant frontier orbitals of thieno[3,2-*b*]benzofuran in Figure 6 correspond to the occupied π type bonding HOMO$_{TF}$ and HOMO$_{TF}$ − 1 orbitals and the lowest unoccupied π type antibonding orbital LUMO$_{TF}$. Thus, applying the FMO theory, the HOMO shape of the π-CO complex is expected to form a combination consisting of bromine LUMO$_{Br}$ and benzothiophene HOMO$_{TF}$ molecular orbital fragments. However, this was not detected. The upper HOMO of π-CO is not formed just from simple HOMO−LUMO interaction, but rather the antibonding upper filled HOMO$_{Br}$ of bromine interacts with the upper HOMO$_{TF}$ of thieno[3,2-*b*]benzofuran forming two filled orbitals, HOMO$_{CO}$ and HOMO$_{CO}$ − 2, in the π-CO complex. In this initial interaction the bromide almost perpendicularly approaches the C(2) atom of the thiophene ring plane. The filled highest π type orbital of thieno[3,2-*b*]benzofuran HOMO$_{TF}$ bearing enhanced electron density on the C(2) atom is directed toward the bromine lone pair

dx.doi.org/10.1021/jp402257u | J. Phys. Chem. A 2013, 117, 8449−8458

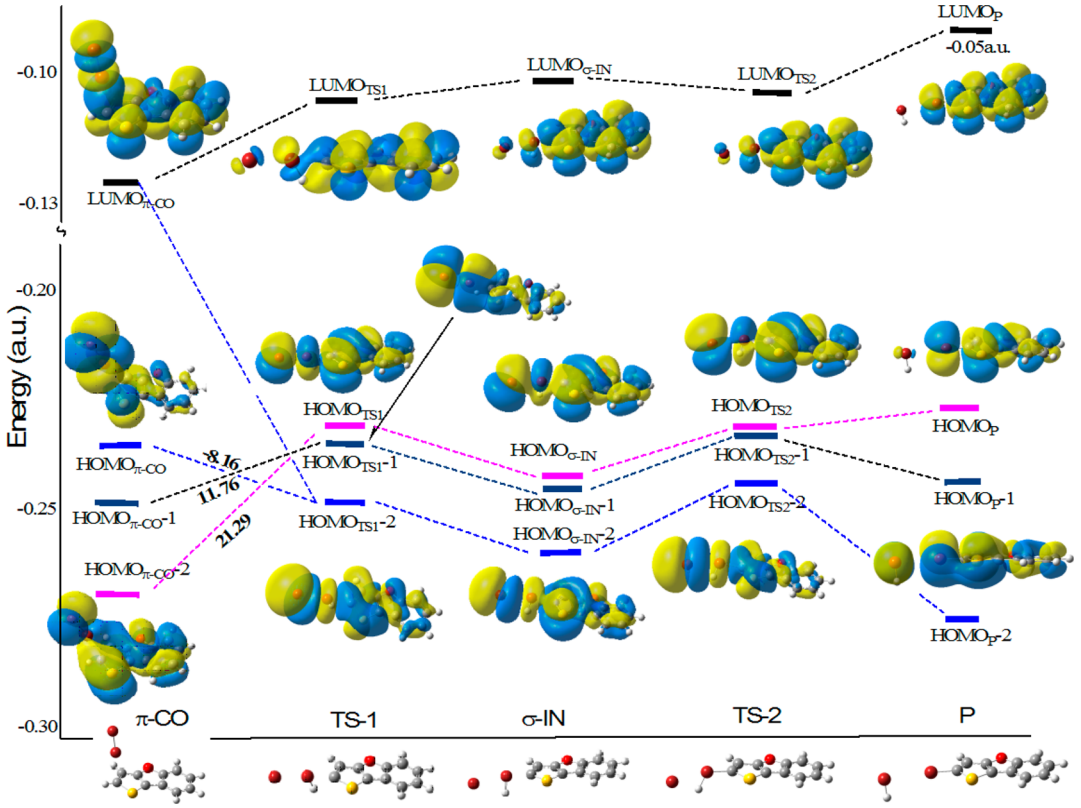

Figure 7. KS molecular orbital transformations during the thieno[3,2-*b*]benzofuran bromination reaction progress along the IRC for the reaction stationary points: π-complex (π-CO), transition state (TS-1), σ-complex intermediate (σ-IN), transition state (TS-2), and reaction products (P). Molecular orbital energy differences in kcal/mol. Single point energy calculations at the B3LYP/6-31++G(d,p) level for the optimized geometries at the B3LYP/6-31+G(d) level.

$HOMO_{Br}$ and increases the overlap between the C(2) atom of the thiophene ring and the bromine orbital. Hereupon it induces mixing of the upper π $HOMO_{TF}$ of TF and the $HOMO_{Br}$ of bromine in the bonding and antibonding manner affording two orbitals of π-CO, $HOMO_{CO}$ and $HOMO_{CO} - 2$, respectively consisting of $HOMO_{Br}$ and $HOMO_{TF}$ molecular orbital fragments. Therewith orbital mixing the π-electron density of $HOMO_{CO}$ flows from the benzofuran fragment to the bromine moiety stabilizing the C(2)−Br bond. Meanwhile the $LUMO_{Br}$ of bromide interacts with the $LUMO_{TF}$ of thieno[3,2-*b*]benzofuran in the bonding and antibonding way affording two lowest unoccupied orbitals of π-CO, $LUMO_{CO}$ and $LUMO_{CO} + 1$, consisting of the $LUMO_{Br}$ and $LUMO_{TF}$ fragments. Other evident MO splittings are also presented in Figure 4. The highest occupied degenerative antibonding filled orbital of bromide $HOMO_{Br} - 1$ interacts with a lower filled $HOMO_{TF} - 1$ of thieno[3,2-*b*]benzofuran in the bonding way and forms $HOMO_{CO} - 2$ of π-CO.

The overall π-CO orbital mixing pattern implies the absence of any accompanying two electron HOMO−LUMO interaction between the upper occupied MOs and high-lying empty orbitals. The examination of molecular orbital electron density plots clearly shows that the initial HOMO−HOMO interaction is involved in the Br and TF interaction at the π-CO stage.

This dominant HOMO−HOMO shape mixing is in agreement with the above-noted considerations based on MO energy splittings. As noted above, the HOMO−HOMO interaction usually dominates in reactions where the initial HOMO−LUMO gap between the reactants is large (>100 kcal/mol). The initial HOMO−LUMO gap for this reaction is 138 kcal/mol, while the approaching reactant HOMOs are close in energy compared to the HOMO−LUMO gap; the energy difference between $HOMO_{Br}$ and $HOMO_{TF}$ is 6.1 kcal/mol. As the reactants approach each other, a high HOMO−LUMO energy gap is reduced by the four electron interactions as the π-CO complex is formed. As a consequence of MO mixing at the π-CO stage, three upper HOMOs are slightly lowered in energy, namely, $HOMO_{CO}$ by 9.6 kcal/mol and $HOMO_{CO} - 2$ by 17.7 kcal/mol. The $LUMO_{CO}$ is strongly lowered in energy by 50.2 kcal/mol, developing π bonding interaction between the bromine and the C(2) atom of the thiophene ring. These splittings evoke the reduction in a HOMO−LUMO energy gap by more than half to 67.15 kcal/mol and facilitate the possibility for the expected two electron interaction that accompanies the molecular interaction between two "nucleophilic" reactants, namely, bromine and thieno[3,2-*b*]benzofuran molecules. Meanwhile, a slight decrease in energy of the highest occupied orbitals of π-CO shows that the first interaction between the reactants is stabilizing. The MO energy changes have an effect upon the total energy of the reacting system. It slightly decreases when the π-CO geometry is formed as compared to that of the reactants R. Moreover, the frontier orbital narrowing represents the readiness for further orbital rearrangements within the system.

As the system moves further from π-CO along the reaction coordinate to σ-IN, the molecular orbital energy level crossings and electron density rearrangements proceed. As a consequence of HOMO−LUMO narrowing at the π-CO complex stage, two electron interactions occur by mixing of $LUMO_{CO}$ and $HOMO_{CO}$ into the $HOMO_{TS-1} - 2$ as the reaction

dx.doi.org/10.1021/jp402257u | J. Phys. Chem. A 2013, 117, 8449−8458

progresses to the transition state TS-1. As illustrated in Figure 7, $HOMO_{TS\text{-}1} - 2$ consists of a mixture of the $LUMO_{CO}$ bromine fragment and the $HOMO_{CO}$ TF fragment. The Br(1)−Br(2) moiety migration toward the C(2) atom of the thiophene ring at this step has an effect upon the frontier MO energy level crossings and electron density rearrangements. As the bromine atom approaches the C(2) atom of the thiophene ring, the out of plane π shaped $HOMO_{CO} - 1$ and $HOMO_{CO}$ transform into the σ in plane shaped HOMOs ($HOMO_{TS1} - 1$ and $HOMO_{TS1} - 2$ accordingly) at the H(1)−C(2)−Br(1) reaction center until the system reaches TS-1 and develops to IN-1. The electron density slightly flows in the opposite direction compared to the π-CO stage, from the bromine fragment to the thiophene ring as shown in $HOMO_{CO}$, $HOMO_{TS\text{-}1} - 2$, and $HOMO_{IN} - 2$ molecular orbital transformations from π-CO to IN-1. The π system development to the in plane shaped σ orbital fragments induces the $HOMO_{CO}$ stabilization by 8.2 kcal/mol in energy as the system goes to TS-1. $HOMO_{CO} - 2$ and $HOMO_{CO} - 1$ are elevated in energy by 11.8 kcal/mol for $HOMO_{CO} - 1$ and 21.3 kcal/mol for $HOMO_{CO} - 2$ as the system reaches the TS-1 transition state. Therefore, in this interaction two lower occupied orbitals of π-CO show an increase in energy to a greater extent than the upper one. This change evokes the MO energy level crossings at this stage. With this the upper π orbital $HOMO_{CO}$ in π-CO was stabilized and took the next lower molecular orbital $HOMO_{TS1} - 2$ position at TS-1, while the two lower $HOMO_{CO} -2$ and $HOMO_{CO} -1$ of π-CO were elevated in energy taking up $HOMO_{TS1}$ and $HOMO_{TS1} - 1$ positions at TS-1. Consequently, two filled MOs are elevated in energy to a greater extent than one HOMO is lowered in energy affording destabilizing interaction. As a result, the free energy of the reacting system at TS-1 increases by 49.4 kcal/mol. The large activation energy barrier can be attributed to the formation of σ bonding interactions in the reaction center H(1)−C(2)−Br(1) before the barrier is crossed.

Further, as the reaction proceeds from the σ bonded σ-IN intermediate to the product, the σ in the plane shaped HOMO fragments transforms into the out of plane π bonded fragments, finally forming a π type bonding between Br(1)−C(2) and H(1)−Br(2) atoms.

4. CONCLUSIONS

Detailed understanding of the thieno[3,2-*b*]benzofuran bromination reaction mechanism has been developed using DFT methods. The variations in charge as well as bond length and bond order have been investigated in the course of the reaction. The frontier π molecular orbitals energy level splittings and shape mixing during the formation of π-complex and its transformation into the σ-complex and final products along the reaction minimal energy path given as intrinsic reaction coordinate have been described. The frontier molecular orbital theory and perturbation molecular orbital theory approaches were used to estimate the π molecular orbital transformations on the reaction minimal energy path.

The bromination of thieno[3,2-*b*]benzofuran proceeds via a mechanism similar to that of electrophilic aromatic substitution. The reaction pathway involves two steps:

1. The π-complex is activated to the σ-complex intermediate. The Br(1)−Br(2) moiety migrates toward the thiophene ring plane with the bromine Br(1) atom heading toward C(2), the interaction changes from π- to a σ-bonding character, and the Gibbs free energy activation barrier of this step is 49.4 kcal/mol in the gas phase and 38.2 kcal/mol for the solvent phase.

2. The σ-complex intermediate transforms into the final products 2-bromothieno[3,2-*b*]benzofuran and HBr. The main structural change of this step is the H(1) migration from the C(2) carbon atom to Br(1) and from Br(1) to Br(2), it accompanies the C(2)−Br(1) bond formation and Br(1)−Br(2) bond disruption, and the Gibbs free energy activation barrier of the second step is 8.1 kcal/mol in the gas phase and 5.1 kcal/mol for the solvent phase.

In the course of reaction, the charge transfer within the Br(1)−Br(2) unit indicates a complicated nature of bonding, which suggests that the reaction may progress via an ionic route. The initial four electron HOMO−HOMO interaction is involved as the π-complex is formed with the effect on the LUMO energy lowering and the HOMO−LUMO energy gap reduction; it facilitates the expected two electron HOMO−LUMO interaction that accompanies the transition state activation for the reaction first step—the π-complex transformation into the σ-complex intermediate.

The solvent type has a significant effect on the reduction of activation energies.

AUTHOR INFORMATION

Corresponding Author

*E-mail: ausra.vektariene@tfai.vu.lt or ausra.vektariene@gmail.com.

Notes

The authors declare no competing financial interest.

ACKNOWLEDGMENTS

The author thanks the Digital Science and Computing Center at Vilnius University for the computational facilities and Dr. Irena Mirvienė for her assistance.

REFERENCES

(1) Chacko, E.; Bornstein, J.; Sardella, D. J. Electronic Structure, Aromatic Character, and Chemical Reactivity of o-Quinonoidal Heterocycles. *J. Am. Chem. Soc.* **1977**, *99*, 8248−8251.

(2) Abbey, E. R.; Zakharov, L. N.; Liu, Sh.-Y. Electrophilic Aromatic Substitution of a BN Indole. *J. Am. Chem. Soc.* **2010**, *132*, 16340−16342.

(3) Hsu, D.-T.; Lin, Ch.-H. Synthesis of Benzo[c] and Naphtho[c]-heterocycle Diesters and Dinitriles via Homoelongation. *J. Org. Chem.* **2009**, *74*, 9180−9187.

(4) Harrison, D. P.; Welch, K. D.; Nicols-Nielander, A. C.; Sabat, M.; Myers, W. H.; Harman, W. D. Efficient Synthesis of an η^2-Pyridine Complex and a Preliminary Investigation of the Bound Heterocycle's Reactivity. *J. Am. Chem. Soc.* **2008**, *130*, 16844−16845.

(5) Joule, J. A.; Mills, K. *Heterocyclic Chemistry*; John Wiley & Sons: New York, 2010.

(6) Rakowski DuBois, M.; Vasquez, L. D.; Ciancanelli, R. F.; Noll, B. C. Electrophilic Substitution of Nitrogen Heterocycles by Molybdenum Sulfide Complexes. *Organometallics* **2000**, *19*, 3507−3515. Kanney, J.; Noll, B. C.; Rakowski DuBois, M. Reactions of Thiiranes and a Thietane with a High Valent Metal Chloride. *Organometallics* **2000**, *19*, 4925−4928.

(7) Liu, F.; Martin-Mingot, A.; Jouannetaud, M.-P.; Zunino, F.; Thibaudeau, S. Superelectrophilic Activation in Superacid HF/SbF5 and Synthesis of Benzofused Sultams. *Org. Lett.* **2010**, *12*, 868−871.

(8) Hajós, G.; Riedl, Z.; Kollenz, G. Recent Advances in Ring Transformations of Five-Membered Heterocycles and Their Fused Derivatives. *Eur. J. Org. Chem.* **2001**, *18*, 3405−3414.

(9) Hill, R. L.; Kardorff, U.; Rack, M.; Got, N.; Baumann, E.; von Deyn, W.; Engel, S.; Mayer, G.; Otten, M.; Rheinheimer, J.; Witschel,

M.; Misslitz, U.; Walter, H.; Westphalen, K. Substituted 4-Benzoylpyrazoles. U.S. Patent 6,028,035, 2000.
(10) Janciene, R.; Stumbreviciute, Z.; Vektariene, A.; Sirutkaitis, R.; Podeniene, D.; Palaima, A.; Puodziunaite, B. Interaction of Derivatives of 7-Amino-1,5-benzo-diazepin-2-ones with α,β-Unsaturated Ketones. *Chem. Heterocycl. Compd. (N. Y., NY, U. S.)* **2010**, *46*, 998−1005.
(11) Janciene, R.; Stumbrevičiūtė, Z.; Vektariene, A.; Kosychova, L.; Klimavičius, A. K.; Palaima, A.; Puodžiūnaitė, B. D. Synthesis of Novel Annelated Systems Based on the Interaction and Reactivity Estimation of Amino-1,5-benzodiazepin-2-ones with Dimethyl-2-oxoglutaconate. *J. Heterocycl. Chem.* **2009**, *46*, 1339−1345. Janciene, R.; Stumbrevičiūtė, Z.; Vektariene, A.; Kosychova, L.; Sirutkaitis, R.; Palaima, A.; Puodziunaite, B. Researches on Thiazolo-benzodiazepines. Behavior of Tetrahydro-1,5-benzodiazepinethiones with Aromatic α-Halogen Ketones. *Hereroat. Chem.* **2008**, *19*, 72−81.
(12) Cernovska, C.; Kosata, B.; Svoboda, J.; Novotna, V. Novel Ferroelectric Liquid Crystals Based on Fused Thieno[3,2-b]furan and Thieno[3,2-b]thiophene Cores. *Liq. Cryst.* **2006**, *33*, 987−996.
(13) Demus, D.; Goodby, J.; Gray, G. W.; Spiess, H.-W.; Vill, V.. *Handbook of Liquid Crystals*; Wiley-VCH: New York, 1998; Vol. 1.
(14) Katritzky, A. R.; Jug, K.; Oniciu, D. C. Quantitative Measures of Aromaticity for Mono-, Bi-, and Tricyclic Penta- and Hexaatomic Heteroaromatic Ring Systems and Their Interrelationships. *Chem. Rev.* **2001**, *101*, 1421−1449.
(15) Iskra, J. *Halogenated Heterocycles Synthesis, Application and Environment*; Springer-Verlag: New York, 2012.
(16) Spcranza, M. Gas-Phase Reactivity of Five-Membered Heteroaromatics toward Electrophiles, An Experimental Check on Theoretical Predictions. *Pure Appl. Chem.* **1991**, *63*, 243−254. Seed, A. Synthesis of Self-Organizing Mesogenic Materials Containing a Sulfur-Based Five-Membered Heterocyclic Core. *Chem. Soc. Rev.* **2007**, *36*, 2046−2069.
(17) Belenkii, L. I.; Suslov, I. A; Chuvylkin, N. D. Substrate and Positional Selectivity in Electrophilic Substitution Reactions of Pyrrole, Furan, Thiophene and Selenophene Derivatives. *Chem. Heterocycl. Compd. (N. Y., NY, U. S.)* **2003**, *39*, 36−48.
(18) Belenkii, L. I.; Kim, T. G.; Suslov, I. A; Chuvylkin, N. D. Substrate and Positional Selectivity in Electrophilic Substitution Reactions in Pyrrole, Furan, Thiophene, And Selenophene Derivatives and Related Benzoannelated Systems. *Russ. Chem. Bull.* **2005**, *54*, 853−863.
(19) Domingo, L. R.; Chamorro, E.; Pérez, P. Understanding the Reactivity of Captodative Ethylenes in Polar Cycloaddition Reactions. A Theoretical Study. *J. Org. Chem.* **2008**, *73*, 4615−4624.
(20) Jaramillo, P.; Domingo, L. R.; Chamorro, E.; Pérez, P. Mechanistic Details of the Domino Reaction of Nitronaphthalenes with the Electron-Rich Dienes. A DFT Study. *J. Mol. Struct.: THEOCHEM* **2008**, *865*, 68−72.
(21) Pérez, P.; Domingo, L. R.; Duque-Noreña, M.; Chamorro, E. A Condensed-to-Atom Nucleophilicity Index. An Application to the Director Effects on the Electrophilic Aromatic Substitutions. *J. Mol. Struct.: THEOCHEM* **2009**, *895*, 86−91.
(22) Alves, C. N.; Carneiro, A. S.; Andrés, J.; Domingo, L. R. A DFT study of the Diels−Alder Reaction between Methyl Acrolein Derivatives and Cyclopentadiene. Understanding the Effects of Lewis Acids Catalysts Based on Sulfur Containing Boron Heterocycles. *Tetrahedron* **2006**, *62*, 5502−5509.
(23) Ghomri, A.; Mekelleche, S. M. Reactivity and Regioselectivity of Five-Membered Heterocycles in Electrophilic Aromatic Substitution: A Theoretical Investigation. *J. Mol. Struct.: THEOCHEM* **2010**, *941*, 36−40.
(24) Mineva, T. T.; Parvanov, V.; Petrov, I.; Neshev, N.; Russo, N. Fukui Indices from Perturbed Kohn−Sham Orbitals and Regional Softness from Mayer Atomic Valences. *J. Phys. Chem. A* **2001**, *105*, 1959−1967. Madjarova, G.; Tadjer, A.; Cholakova, Tz. P.; Dobrev, A. A.; Mineva, T. Selectivity Descriptors for the Michael Addition Reaction as Obtained from Density Functional Based Approaches. *J. Phys. Chem. A* **2005**, *109*, 387−393.
(25) Svoboda, J.; Pihera, P.; Sedmera, P.; Palecek, J. Electrophilic Substitution Reactions of [1]Benzothieno[3,2-b]furan. *Collect. Czech. Chem. Commun.* **1996**, *61*, 888−900.
(26) Vachal, P.; Pihera, P.; Svoboda, J. Thieno[3,2-b]benzofuran—Synthesis and Reactions. *Collect. Czech. Chem. Commun.* **1997**, *62*, 1468−1480.
(27) Vektariene, A.; Vektaris, G.; Svoboda, J. A Theoretical Approach to the Nucleophilic Behavior of Benzofused Thieno[3,2-b]furans Using DFT and HF Based Reactivity Descriptors. *ARKIVOC (Gainesvill, FL, U. S.)* **2009**, *7*, 311−329.
(28) Truhlar, D. G.; Garrett, B. C.; Klippenstein, S. J. Current Status of Transition-State Theory. *J. Phys. Chem.* **1996**, *100*, 12771−12800.
(29) Fukui, K. Formulation of the Reaction Coordinate. *J. Phys. Chem. A* **1970**, *74*, 4161−4163.
(30) Gonzalez, C.; Schlegel, H. B. An Improved Algorithm for Reaction Path Following. *J. Chem. Phys.* **1989**, *90*, 2154−2161.
(31) Rauk, A. *Orbital Interaction Theory of Organic Chemistry*; John Wiley & Sons: New York, 2001.
(32) Ogino, T.; Watanabe, T.; Matsuura, M.; Watanabe, Ch.; Ozaki, H. Semiquantitative FMO Analysis of Substituent Effect on the Reaction of Permanganate Ion with Unsymmetrical Alkenes. *J. Org. Chem.* **1998**, *63*, 2627−2633.
(33) Spino, C.; Rezaei, H.; Dory, Y. L. Characteristics of the Two Frontier Orbital Interactions in the Diels−Alder Cycloaddition. *J. Org. Chem.* **2004**, *69*, 757−764.
(34) Bach, R. D.; Wolber, G. J.; Schlegel, H. B. The Origin of the Barriers to Thermally Allowed, Six-Electron, Pericyclic Reactions: The Effect of HOMO-HOMO Interactions on the Trimerization of Acetylene. *J. Am. Chem. Soc.* **1985**, *107*, 2837−2841.
(35) Bach, R. D.; Wolber, G. J. Nucleophilic Substitution at Vinylic Carbon. The Importance of the HOMO-HOMO Interaction. *J. Am. Chem. Soc.* **1984**, *106*, 1401−1409.
(36) Bach, R. D.; Wolber, G. J. The Mechanism of Oxygen Transfer from Oxaziridine to Ethylene: The Consequence of HOMO-HOMO Interactions on Frontier Orbital Narrowing. *J. Am. Chem. Soc.* **1984**, *106*, 1410−1415.
(37) Bach, R. D.; McDouall, J. J. W.; Schlegel, H. B.; Wolber, G. J. Electronic Factors Influencing the Activation Barrier of the Diels-Alder Reaction. An Ab Initio Study. *J. Org. Chem.* **1989**, *54*, 2931−2935.
(38) Bach, R. D.; Coddens, B. A.; McDouall, J. J. W.; Schlegel, H. B.; Davis, F. A.The Mechanism of Oxygen Transfer from an Oxaziridine to a Sulfide and a Sulfoxide: A Theoretical Study. *J. Org. Chem.* **1990**, *55*, 3325−3330.
(39) Libit, L.; Hoffmann, R. Detailed Orbital Theory of Substituent Effects. Charge Transfer, Polarization, and the Methyl Group. *J. Am. Chem. Soc.* **1974**, *96*, 1370−1383.
(40) Inagaki, S.; Fujimoto, H.; Fukui, K. Orbital Interaction in Three Systems. *J. Am. Chem. Soc.* **1976**, *98*, 4693−4701.
(41) Frisch, M. J.; Trucks, G. W.; Schlegel, H. B.; Scuseria, G. E.; Robb, M. A.; Cheeseman, J. R.; Montgomery, J. A., Jr.; Vreven, T.; Kudin, K. N.; Burant, J. C.; et al. *Gaussian 03*, revision C.02; Gaussian Inc.: Wallingford, CT, 2004.
(42) Sousa, S. F.; Fernandes, P. A.; Ramos, M. J. General Performance of Density Functionals. *J. Phys. Chem. A* **2007**, *111*, 10439−10452.
(43) Morgado, C. A.; McNamara, J. P.; Hillier, I. H.; Burton, N. A.; Vincent, M. A. Density Functional and Semiempirical Molecular Orbital Methods Including Dispersion Corrections for the Accurate Description of Noncovalent Interactions Involving Sulfur-Containing Molecules. *J. Chem. Theory Comput.* **2007**, *3*, 1656−1664.
(44) Martınez, A.; Vazquez, M. V.; Carreo-Macedo, J. L.; Sansores, L. E.; Salcedo, R. Benzene Fused Five-Membered Heterocycles. A Theoretical Approach. *Tetrahedron* **2003**, *59*, 6415−6422.
(45) Nathaniel, R.; Mineva, T.; Nikolova, R.; Bojilova, A. Density Functional Study of the Interaction of 3-(ω-Bromoacetyl)coumarin with Phosphites. *Int. J. Quantum Chem.* **2006**, *106*, 1357−1366.
(46) Vektariene, A.; Vektaris, G. Quantum Chemical Estimation of Reactivity of 2,3,4,5-Tetrahydro-1,5-benzodiazepin-2(1H)-ones in

Electrophilic Aromatic Substitution. *Heteroat. Chem.* **2004**, *15*, 263−270.
(47) Janciene, R.; Vektariene, A.; Stumbriaviciute, Z.; Kosychova, L.; Klimavicius, A.; Puodziunaite, B. A. Straightforward Synthesis of Novel 4H-Thiazolo[3,2-d][1,5]benzodiazepine Derivatives. *Heteroat. Chem.* **2004**, *15*, 363−368.
(48) Vektariene, A.; Vektaris, G.; Rankin, D. W. H. DFT Study of the Regioselectivity of Addition of Sulfenylchloride to Ethenes. *Heteroat. Chem.* **2007**, *18*, 695−703.
(49) Janciene, R.; Vektariene, A.; Stumbreviciute, Z.; Puodziunaite, B. D. Experimental and Theoretical Investigation of Substituent Effects in a Two-Pathway Reaction of Tetrahydro-1,5-benzodiazepine-2-thiones with 4-Substituted 2-Bromoacetophenones. *Monatsh. Chem.* **2011**, *142*, 609−618.
(50) Choe, S. J. Comparison of Different Theory Models and Basis Sets in Calculations of TPOP24N-Oxide Geometry and Geometries of meso-Tetraphenyl Chlorin N-Oxide Regioisomers. *Bull. Korean Chem. Soc.* **2012**, *33*, 2861−2866.
(51) Carlson, H., A.; Nguyen, T. B.; Orozco, M.; Jorgensen, W. L. Accuracy of Free Energies of Hydration for Organic Molecules from 6-31G* Derived Partial Charges. *J. Comput. Chem.* **2004**, *14*, 1240−1249.
(52) Rassolov, V. A.; Ratner, M. A.; Pople, J. A.; Redfern, P. C.; Curtiss, L. A. 6-31G* Basis Set for Third-Row Atoms. *J. Comput. Chem.* **2001**, *22*, 976−984.
(53) Islam, S. M.; Poirier, R. A. New Insights into the Bromination Reaction for a Series of Alkenes. A Computational Study. *J. Phys. Chem. A* **2007**, *111*, 13218−13232. Islam, S. M.; Huelin, S. D.; Dawe, M.; Poirier, R. A. Comparison of the Standard 6-31G and Binning-Curtiss Basis Sets for Third Row Elements. *J. Chem. Theory Comput.* **2008**, *4*, 86−100.
(54) Halgren, T. A.; Lipscomb, W. N. The Synchronous-Transit Method for Determining Reaction Pathways and Locating Molecular Transition States. *Chem. Phys. Lett.* **1977**, *49*, 225−232.
(55) Cancès, E.; Mennucci, B.; Tomasi, J. A New Integral Equation Formalism for the Polarizable Continuum Model: Theoretical Background and Applications to Isotropic and Anisotropic Dielectrics. *J. Chem. Phys.* **1997**, *107*, 3032.
(56) Mennucci, B.; Cancès, E.; Tomasi, J. Evaluation of Solvent Effects in Isotropic and Anisotropic Dielectrics and in Ionic Solutions with a Unified Integral Equation Method: Theoretical Bases, Computational Implementation, and Numerical Applications. *J. Phys. Chem. B* **1997**, *101*, 10506−10517.
(57) Trummal, A.; Rummel, A.; Lippmaa, E.; Burk, P.; Koppel, I. A. IEF-PCM Calculations of Absolute pKa for Substituted Phenols in Dimethyl Sulfoxide and Acetonitrile Solutions. *J. Phys. Chem. A* **2009**, *113*, 6206−6212.
(58) Gonzalez, C.; Schlegel, H. B. An Improved Algorithm for Reaction Path Following. *J. Chem. Phys.* **1989**, *90*, 2154−2161.
(59) Peterson, T. H.; Carpenter, B. K. Estimation of Dynamic Effects on Product Ratios by Vectorial Decomposition of a Reaction Coordinate. Application to Thermal Nitrogen Loss from Bicyclic Azo Compounds. *J. Am. Chem. Soc.* **1992**, *114*, 766−767.
(60) Reed, A. E.; Curtiss, L. A.; Weinhold, F. Intermolecular Interactions from a Natural Bond Orbital, Donor-Acceptor Viewpoint. *Chem. Rev.* **1988**, *88*, 899−926.
(61) Pierre, H.; Kohn, W. Inhomogeneous Electron Gas. *Phys. Rev.* **1964**, *136* (3B), 864−871.
(62) Kohn, W.; Sham, L. J. Self-Consistent Equations Including Exchange and Correlation Effects. *Phys. Rev.* **1965**, *140* (4A), 1133−1138.
(63) Lide, D. R. *Handbook of Chemistry and Physics: A Ready-Reference Book of Chemical and Physical Data*; CRC Press: Boca Raton, FL, 2008.
(64) Vittadini, A.; Casarin, M.; Selloni, A. Chemistry of and on TiO2 Anatase Surfaces by DFT Calculations: A Partial Review. *Theor. Chem. Acc.* **2007**, *117* (5−6), 663−671.
(65) Bickelhaupt, F. M.; Baerends, E. J. Kohn-Sham Density Functional Theory: Predicting and Understanding Chemistry. *Rev. Comput. Chem.* **2000**, *15*, 1−86.
(66) Hoffmann, R. Building Bridges between Inorganic and Organic Chemistry (Nobel Lecture). *Angew. Chem., Int. Ed. Engl.* **1982**, *21*, 711−724.
(67) Hoffmann, R. *Solids and Surfaces: A Chemists View of Bonding in Extended Structures*; VCH: Weinheim, Germany, 1988.
(68) Hoffmann, R.; Woodward, R. B. Conservation of Orbital Symmetry. *Acc. Chem. Res.* **1968**, *1*, 17−22.
(69) Fujimoto, H.; Mizutani, Y.; Iwase, K. An Aspect of Substituents and Peripheral Structures in Chemical Reactivities of Molecules. *J. Phys. Chem.* **1986**, *90*, 2768−277.
(70) Fujimoto, H. Paired Interacting Orbitals: A Way of Looking at Chemical Interactions. *Acc. Chem. Res.* **1987**, *20*, 448−453.
(71) Fujimoto, H.; Satoh, Sh. Orbital Interactions and Chemical Hardness. *J. Phys. Chem.* **1994**, *98*, 1436−1441.
(72) Rodrigo, R. S.; Ramalho, T. C.; Santos, J. M.; Figueroa-Villar, J. D. On the Limits of Highest-Occupied Molecular Orbital Driven Reactions: The Frontier Effective-for-Reaction Molecular Orbital Concept. *J. Phys. Chem. A* **2006**, *110*, 1031−1040.
(73) Zevallos, J. A.; Toro-Labbé, A. A Theoretical Analysis of the Kohn-Sham and Hartree-Fock Orbitals and Their Use in the Determination of Electronic Properties. *J. Chil. Chem. Soc.* **2003**, *48* (4), 39−47.
(74) Stowasser, R.; Hoffmann, R. What Do the Kohn-Sham Orbitals and Eigenvalues Mean? *J. Am. Chem. Soc.* **1999**, *121*, 3414−3420.
(75) Tee, O. S.; Paventi, M.; Bennett, J. M. Kinetics and Mechanism of the Bromination of Phenols and Phenoxide Ions in Aqueous Solution. Diffusion-Controlled Rates. *J. Am. Chem. Soc.* **1989**, *111*, 2233−2240.
(76) Schubert, W. M.; Dial, J. K. Two-Step Mechanism of Noncatalytic Aromatic Bromination. Controlled Variation of the Rate-Controlling Step. *J. Am. Chem. Soc.* **1975**, *97*, 3877−3878.
(77) Keefer, R. M.; Andrews, L. J. Halogen Order in the Kinetics of Bromination of Poly(Methylbenzenes) in 90% Aqueous Acetic Acid. *J. Am. Chem. Soc.* **1977**, *99*, 5693−5695.